Coupled-cluster approach for studying the singlet and triplet exciton formation rates in conjugated polymer LED's

A. Ye,[1] Z. Shuai,[1] and J. L. Brédas[1,2]
[1]*Centre de Recherche en Electronique et Photonique Moléculaires, Service de Chimie des Matériaux Nouveaux, Université de Mons-Hainaut, Place du Parc 20, B-7000 Mons, Belgium*
[2]*Department of Chemistry, The University of Arizona, 1306 East University Boulevard, Tucson, Arizona 85721-0041*
(Received 30 May 2001; published 10 January 2002)

The coupled-cluster equation of motion approach is applied to describe positively and negatively charged states as well as exciton states in conjugated polymers. The formation rates for singlet and triplet excitons associated with intermolecular charge-transfer processes are calculated. It is found that the interchain bond-charge correlation has a strong influence on the singlet/triplet ratio, since the charge-transfer configuration contributes differently to the singlet and triplet excitons. In addition, we find that the range of electron interaction potential has a strong influence on the formation rates. The ratio between the electroluminescence and photoluminescence quantum yields can exceed the 25% spin-degeneracy statistical limit.

DOI: 10.1103/PhysRevB.65.045208 PACS number(s): 78.60.Fi, 72.80.Le, 71.35.−y, 31.15.Dv

I. INTRODUCTION

Electroluminescence (EL) in conjugated polymers has attracted wide interest because of the huge potential for application in display devices.[1–3] Polyparaphenylene vinylene (PPV) and its derivatives are among the prominent polymeric materials to demonstrate high EL efficiency. The semiconducting nature of conjugated polymers comes from the delocalized π-electron bonding along the polymer chain.

A polymer light-emitting-diode (LED) device usually consists of a layer of a luminescent organic conjugated polymer sandwiched between two metal electrodes. Switching the device on results in the injection of electrons and holes from the electrodes into the polymer layer. The charge carriers then migrate through the organic layer, usually via interchain hopping processes, and eventually recombine to form intrachain excitons. The radiative decay of singlet excitons gives rise to emission of photons, i.e., luminescence.

The quantum efficiency for EL is defined as the ratio of the number of exciton formation events within the device to the number of electrons flowing in the external circuit. It can be expressed as a product of three factors $\eta_{\mathrm{EL}}=\eta_1\eta_2\eta_3$, where η_1 is the ratio of the number of emitted photons over the number of optically active singlet excitons, i.e., the efficiency of radiative decay of the singlet excitons; η_2 is the ratio of the number of optical excitons over the total number of excitons, i.e., the fraction of excitons which are formed as singlets; and η_3 is the ratio of the number of excitons within the device over the number of injected carriers, it is the probability for carrier recombination giving rise to intramolecular excitons. Since the singlet excitons can decay both radiatively and nonradiatively, $\eta_1<1$. The PL quantum efficiency can be also decomposed as $\eta_{\mathrm{PL}}=\eta_1\eta_4$, where η_1 has the same meaning as for EL and η_4 is the ratio of the number of optical excitons over the number of absorbed photons. As observed by Harrison *et al.*, almost all the photons absorbed by a PPV film convert to excitons, which implies that $\eta_4\sim 1$.[4,5] Since $\eta_3<1$, we have $\eta_{\mathrm{EL}}/\eta_{\mathrm{PL}}(=\eta_2\eta_3/\eta_4)<\eta_2$.

On the basis of simple spin multiplicity statistics, it is often stated that $\eta_2=\frac{1}{4}$, i.e., the EL efficiency is limited to 25% of that of photoluminescence (PL). Since the recombination of an electron and hole (both spin $\frac{1}{2}$) pair leads to four microstates in total with three triplet states and one singlet state and only singlet states contribute to the spin-allowed radiative emission.[6,7] Recently, Cao *et al.* found that the ratio of quantum efficiencies of EL with respect to PL in a substituted PPV-based LED can reach a value as high as 50%.[8] Ho *et al.* have also fabricated an efficient device for which they obtain that $\eta_2\geqslant 0.35-0.45$.[9] Wohlgenannt *et al.* have been able to measure directly $\sigma_{S/T}$ by using a spin-dependent recombination technique for a large number of π-conjugated polymers and oligomers. In all cases, they find that the experimental $\sigma_{S/T}$ values are significantly larger than 1, thus $\eta_2>0.25$.[10]

In a previous study, we briefly described theoretically a microscopic mechanism of interchain bond-charge correlation that was able to explain the violation of the $\frac{1}{4}$ statistics.[11] In this work, we develop a more accurate method and provide a more detailed description. We note that Kobrak and Bittner have developed a methodology based on the particle-hole picture of solid-state physics, that allows the simulation of the vibronic dynamics of a one-dimensional polymer system.[12–14] They extended this formalism and carried out quantum molecular dynamics simulations of the formation of exciton states from polarons. They evaluated the cross sections for the formation of singlet and triplet excitons as a function of exciton binding energy and strength of the applied voltage bias.[15] This basically corresponds to an intrachain dynamical mechanism. Their theoretical results confirmed that the 25% spin-degeneracy statistical limit is invalid.

Cao *et al.* attributed the violation of the 25% limit to be a consequence either of a small exciton binding energy or a higher cross section for an electron-hole pair to form a singlet bound state than to form a triplet. Since the splitting between the lowest singlet and triplet excitons is around 0.6–0.7 eV in PPV,[15] this appears to prevent any possible contribution from thermalized triplet excitons to the

luminescence,[16] which favors the second alternative. We note that the cross section of a singlet is about 20 times as a large as that of a triplet in the low-energy scattering process of neutrons with protons (both have spin $\frac{1}{2}$).[17] Thus, we can expect a scenario according to which the formation rates for singlet and triplet excitons from free electron-hole pairs (both also have spin $\frac{1}{2}$) can be different. If it is easier for the singlet pair to bind than the triplet pair, then η_2 is not necessarily equal to 25% and the ratio of EL to PL efficiency can go beyond the 25% limit.[11] Considering the difference between the cross sections for singlet and triplet states, the expression for η_2 discussed above should be written as

$$\eta_2=\sigma_S/(\sigma_S+3\sigma_T)=\sigma_{S/T}/(\sigma_{S/T}+3), \tag{1}$$

where $\sigma_{S(T)}$ is the cross section for singlet (triplet) formation and $\sigma_{S/T}=\sigma_S/\sigma_T$. For $\sigma_S=\sigma_T$, we get $\eta_2=25\%$, the statistical limit; for $\sigma_S=3\sigma_T, \eta_2=50\%$; for $\sigma_T=0, \eta_2=100\%$.

In our previous work,[11] we calculated the formation probabilities of singlet and triplet excitons within a single configuration interaction (SCI) approach. In order to obtain more accurate results, we consider a more sophisticated model based on the coupled-cluster method. The coupled-cluster method (CCM) has been shown to provide accurate descriptions of electron correlation in many-body systems.[18,19] Bartlett and co-workers have widely extended the application scope of CCM to quantum chemistry.[20,21] CCM, specifically CCSD (single and double excitations), is size consistent, numerically efficient, and applicable to a wide range of problems within a single framework.

We first give in Sec. II a brief description of the coupled-cluster equation of motion (CCSD-EOM) approach for charged states and exciton states. In Sec. III, we will present a two-chain model to calculate the singlet and triplet exciton formation rates via interchain charge-transfer (CT) processes. Finally, the results and discussion are given in Sec. VI.

II. COUPLED-CLUSTER EQUATION-OF-MOTION METHOD

The CCSD-EDM approach[22] is used to describe the ground state, positively and negatively charged states, and exciton states of a conjugated polymer chain. We have shown that this approach can provide a very accurate description of the electronic structure and optical properties. Here, we give a brief overview of this method.

We adopt the following convention: indices $i,j,k,l,\ldots$, refer to occupied molecular orbitals (MO's); $a,b,c,d,\ldots$ to virtual MO's and p,q,r,s to generic MO's. The general electronic Hamiltonian for a molecule is expressed as

$$H=\sum_{pq} h_{pq}p^+q+\frac{1}{4}\sum_{pqrs}\langle pq\|rs\rangle p^+q^+sr. \tag{2}$$

The first term is the one-electron part, which includes electron kinetic energy and electron nuclear interaction. The second term, the two-electron part, is given in the antisymmetric form $\langle pq\|rs\rangle=\langle pq|rs\rangle-\langle pq|sr\rangle$ and the two-electron integral is defined as

$$\langle pq|rs\rangle=\int\int dr_1dr_2\varphi_p^*(r_1)\varphi_q^*(r_2)\frac{1}{r_{12}}\varphi_r(r_1)\varphi_S(r_2) \tag{3}$$

with φ denoting the molecular orbital wave function.

A. Ground state

The CCSD ground-state ansatz has been proposed as[18,19]

$$|CC\rangle=\exp(T)|\mathrm{HF}\rangle, \tag{4}$$

where $|\mathrm{HF}\rangle$ is the Hartree-Fock (HF) ground-state determinant obtained by self-consistent field iteration; T consists of a linear combination of the single and double excitations:

$$T=T_1+T_2=\sum_{ia} t_i^a a^+i+\sum_{\substack{i>i\\a>b}} t_{ij}^{ab}a^+ib^+j,$$

with the t's being the amplitudes of the excitation configurations. The ground state is obtained by solving the following Schrödinger equations:

$$H|\mathrm{HF}\rangle=E_{HF}|\mathrm{HF}\rangle,$$

$$H\exp(T)|\mathrm{HF}\rangle=E_{CC}\exp(T)|\mathrm{HF}\rangle. \tag{5}$$

In order to evaluate physically measurable quantities, we also need the left eigenvector of the CCSD ground state, i.e., the so-called Λ state in CCSD gradient theory,[23] which is defined as

$$\langle L_0|=\langle\mathrm{HF}|(1+\Lambda)\exp(-T),$$

where

$$\Lambda=\sum_{ia}\lambda_a^i i^+a+\sum_{\substack{i>j\\a>b}}\lambda_{ab}^{ij}i^+aj^+b$$

is the de excitation operator. The amplitude λ is determined by the Schrödinger equation of the Λ state

$$\begin{aligned}\langle L_0|H&=\langle\mathrm{HF}|(1+\Lambda)\exp(-T)H\\&=\langle\mathrm{HF}|(1+\Lambda)\exp(-T)E_{\mathrm{CC}}.\end{aligned} \tag{6}$$

B. Excited states

Based on the CCSD ground state, we can construct the configuration space by promoting one and two electrons from occupied to virtual MO's. We denote the excitation operators as $|\tau\rangle=\{c^+k, c^+kd^+l\}$. The excited-state wave function is constructed as a linear combination of all the single and double excitations on the CCSD ground state

$$|\mathrm{ex}\rangle=\sum_\tau R_\tau\exp(T)|\tau\rangle, \tag{7a}$$

$$\langle\mathrm{ex}|=\sum_\tau\langle\tau|L_\tau\exp(-T), \tag{7b}$$

where $|\tau\rangle = \tau|\mathrm{HF}\rangle$ represents an excitation determinant and R_τ is the corresponding coefficient to be determined. The excited-state Schrödinger equation becomes

$$H|\mathrm{ex}| = E|\mathrm{ex}\rangle; \quad H\sum_\tau R_\tau \exp(T)|\tau\rangle = E\sum_\tau R_\tau \exp(T)|\tau\rangle, \tag{8}$$

where E is the excited state energy. When multiplying the above equation by $\exp(-T)$ from the left and then by an excitation ket configuration $\langle\omega|$, we obtain the following eigen-equation:

$$\sum_\omega \bar{H}_{\tau\omega} R_\omega = E R_\omega$$

or

$$\sum_\omega (\bar{H}_{\tau\omega} - E_{\mathrm{CC}}\delta_{\tau\omega}) R_\omega = (E - E_{\mathrm{CC}}) R_\tau, \tag{9}$$

where E_{CC} is the CCSD ground state energy, and

$$\begin{aligned}\bar{H} &= \exp(-T) H \exp(T) \\ &= H + [H,T] + \frac{1}{2}[[H,T],T] \\ &\quad + \frac{1}{6}[[[H,T],T],T] + \frac{1}{24}[[[[H,T],T],T],T]\end{aligned} \tag{10}$$

is the Hausdorff similarity transformed Hamiltonian, and $\bar{H}_{\tau\upsilon} - E_{\mathrm{CC}}\delta_{\tau\upsilon}$ is referred to as the Jacobian. In principle, the expansion is infinite. However, in CCSD, T is truncated at the double-excitation level, and the Hamiltonian is at most two-body term, which contains a product of four generic fermion operators. Each commutation $[H,T]$ replaces the generic operator by a specific operator from excitation T. Then the Hausdorff transformation terminates exactly after five terms, since all the excitation operators commute.

Since the Jacobian is no longer Hermitian, for each eigenvalue there exist a right eigenvector and a left eigenvector. The left eigenvector is expressed as

$$\langle \mathrm{ex}| = \sum_\tau \langle\mu| L_\tau \exp(-T). \tag{11}$$

L_τ can be determined in a similar way as R_τ.

C. Charged states

Positively charged state. When an electron is extracted from a chain, we can obtain the eigenstates by mapping the Hamiltonian into a configuration subspace of the type $|\sigma\rangle = \{n, g^+ no\}$, where indices n,o refer to occupied MO's and g refers to a virtual MO. Then the eigenstates can be expressed as

$$|p\rangle = \sum_\sigma X_\sigma \exp(T)|\sigma\rangle, \tag{12a}$$

$$\langle p| = \sum_\sigma \langle\sigma| Y_\sigma \exp(-T). \tag{12b}$$

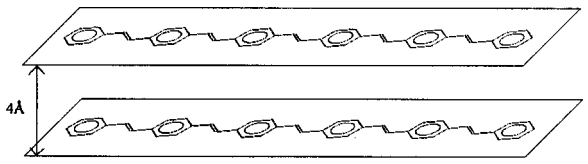

FIG. 1. Sketch of the two-chain model considered in this work.

To derive the eigenequation, we insert Eq. (12a) into the Schrödinger equation and extract the CC ground-state energy

$$(H - E_{\mathrm{CC}})|p\rangle = (E - E_{\mathrm{CC}})|p\rangle, \tag{13}$$

we obtain

$$(H - E_{\mathrm{CC}})\sum_\sigma X_\sigma \exp(T)|\sigma\rangle = (E - E_{\mathrm{CC}})\sum_\sigma X_\sigma \exp(T)|\sigma\rangle. \tag{14}$$

When multiplying the above equation by $\exp(-T)$ from the left and then by $\langle\sigma|$, the following eigenequation is derived:

$$\sum_\rho (\bar{H}_{\sigma\rho} - E_{\mathrm{CC}}\delta_{\sigma\rho}) X_\rho = \Delta E X_\sigma, \tag{15}$$

where $\Delta E = E - E_{\mathrm{CC}}$ is the ionization potential (IP). The eigenequation for Y_σ is obtained in the same way

$$\sum_\sigma Y_\sigma (\bar{H}_{\sigma\rho} - E_{\mathrm{CC}}\delta_{\sigma\rho}) = \Delta E Y_\rho. \tag{16}$$

The expressions for the matrix elements $\bar{H}_{\sigma\rho}$ are somewhat complex and detailed in the Appendix.

Negatively charged state. When adding an electron to a neutral closed shell, we can construct the configuration space as $|\nu\rangle = \{e^+, e^+ f^+ m\}$, where index m refers to occupied MO's and e,f refer to virtual MO's. Then, the eigenstates are expanded within this subspace as

$$|n\rangle = \sum_\nu U_\nu \exp(T)|\nu\rangle, \quad \langle n| = \sum_\nu \langle\nu| V_\nu \exp(-T). \tag{17}$$

For the negatively charged states, we write the eigenequations for U_ν and V_ν:

$$\sum_\mu (\bar{H}_{\mu\nu} - E_{\mathrm{CC}}\delta_{\mu\nu}) U_\mu = \Delta E' U_\nu, \tag{18}$$

$$\sum_\nu V_\mu (\bar{H}_{\mu\nu} - E_{\mathrm{CC}}\delta_{\mu\nu}) = \Delta E' Y_\nu, \tag{19}$$

where $\Delta E' = E - E_{\mathrm{CC}}$ is the electron affinity (EA) and the expressions for the matrix elements $\bar{H}_{\mu\nu}$ are given in the Appendix.

III. DESCRIPTION OF THE MODEL

We consider a system consisting of two PPV oligomers whose molecular planes are parallel and separated by a distance of 4 Å, see Fig. 1. Suppose that initially one chain

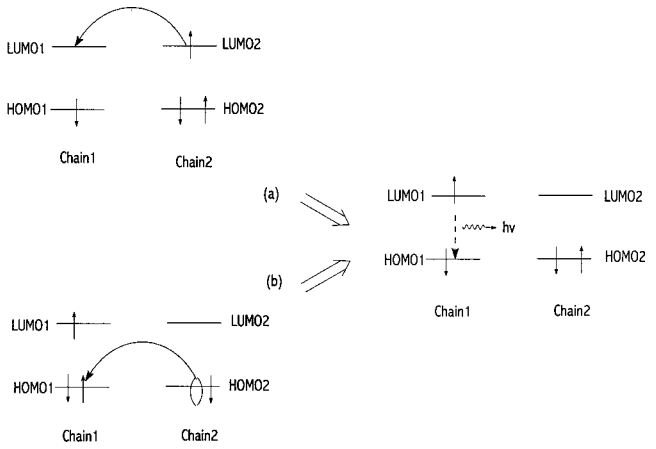

FIG. 2. Illustration of the recombination scenario treated in our model; we only depict the singlet configuration.

carries a positive charge and the other a negative charge (to mimic the charge injection process in LED's. The initial states are $|in\rangle=|n_2\rangle|p_1\rangle$ (or $|n_1\rangle|p_2\rangle$), where $|n\rangle$ represents the negatively charged state and $|p\rangle$ represent the positively charged state. This ''free'' charge pair can be either in a triplet or a singlet configuration. Through a charge-transfer process, this pair can recombine and form an exciton. The final states are $|fi\rangle=|gs_2\rangle|ex_1\rangle$ (or $|gs_1\rangle|ex_2\rangle$). We assume that the total spin is a good quantum number, i.e., the singlet or triplet ''free'' pairs only form singlet or triplet excitons as the final state. This scenario is shown in Fig. 2, in which we only depict the singlet configuration.

The conjugated system is described by the Pariser-Parr-Pople model

$$H=-\sum_{\langle\mu\nu\rangle s} t_{\mu\nu}(c_{\mu s}^{+}c_{\nu s}+\text{h.c.})+U\sum_{\mu} n_{\mu\uparrow}n_{\mu\downarrow} + \sum_{\mu<\nu} V(r_{\mu\nu})n_{\mu}n_{\nu}. \tag{20}$$

The first term represents the π-electron (with spin s) hopping integral ($t_{\mu\nu}$) between nearest-neighbor carbon sites; the second and third terms are the electron-electron diagonal density-density interactions

$$n_{\mu s}=c_{\mu s}^{+}c_{\mu s}, \quad n_{\mu}=\sum_{s} n_{\mu s}.$$

The long range interactions for the π-electrons of conjugated carbon systems is described by the Ohno-Klopman potential with $U=11.13$ eV (Refs. 24 and 25)

$$V(r)=\frac{U}{\sqrt{1+0.5976(\varepsilon r)^2}}, \tag{21}$$

where r is the internuclear distance (in Å). The Ohno-Klopman original parameters corresponds to $\varepsilon=1$. For $\varepsilon>1$, the potential represents a more localized screened interaction.

The hopping integrals are set to standard values: within the vinylene linkage, $t_s=-2.2$ eV for the single bonds (1.46 Å) and $t_d=-2.6$ eV for the double bonds (1.35 Å); in the phenylene rings, all integrals are set to $t_b=-2.4$ eV. We then introduce a general interchain coupling term

$$H'=\sum_{pq} h_{pq}p^{+}q+\frac{1}{4}\sum_{pqrs}\langle pq\|rs\rangle p^{+}q^{+}sr. \tag{22}$$

Each term has mixing of chain 1 and chain 2 spin-orbital indices; h_{pq} is the hopping integral, in the MO representation

$$h_{pq}=\sum_{\alpha_1\beta_2} t^{\perp}(\alpha_1,\beta_2)\Psi_{p\alpha_1}\Psi_{q\beta_{21}}, \tag{23}$$

$$\langle pq|rs\rangle=\sum_{\alpha\beta\gamma\eta}\Psi_{p\alpha}\Psi_{q\beta}\Psi_{r\gamma}\Psi_{s\eta}[\alpha\gamma|\beta\eta]. \tag{24}$$

Ψ is the LCAO coefficient of the one-electron wave function and $[\alpha\gamma|\beta\eta]$ is the Coulomb integral in the site representation.

We then apply the Fermi golden rule to calculate the exciton formation rate

$$|\langle \text{in}|H'|\text{fi}\rangle|^2=\frac{\langle \text{in}|H'|\text{fi}\rangle\langle \text{fi}|H'|\text{in}\rangle}{\langle \text{in}|\text{in}\rangle\langle \text{fi}|\text{fi}\rangle},$$

where $|\text{in}\rangle$ and $|\text{fi}\rangle$ represent the initial and final states, respectively. There are two kinds of initial states and final states:

$$|\text{in}_1\rangle=(|n_2\rangle_{\uparrow}|p_1\rangle_{\downarrow}\pm|n_2\rangle_{\downarrow}|p_1\rangle_{\uparrow})/\sqrt{2}, \tag{25a}$$

$$|\text{in}_2\rangle=(|p_2\rangle_{\uparrow}|n_1\rangle_{\downarrow}\pm|p_2\rangle_{\downarrow}|n_1\rangle_{\downarrow})/\sqrt{2}, \tag{25b}$$

$$|\text{fi}_1\rangle=|\text{ex}_1||\text{gs}_2\rangle, \tag{25c}$$

$$|\text{fi}_2\rangle=|\text{ex}_2\rangle|\text{gs}_1\rangle. \tag{25d}$$

The ground state $|\text{gs}\rangle$, negatively charged states $|n\rangle$, positively charged states $|p\rangle$, and exciton states $|\text{ex}\rangle$ are obtained via the CCSD-EOM approach described in the previous section, indices 1,2 refer to chain 1,2, and $+/-$ is for singlet/triplet. It can be seen that $\langle \text{in}_1|H'|\text{fi}_1\rangle$ is the rate of exciton formed on chain 1 through electron transfer, $\langle \text{in}_1|H'|\text{fi}_2\rangle$ is exciton formation on chain 2, etc. We find that for the two-body interchain coupling, the only relevant integral is of the type $[11|12]$ or $[22|21]$, i.e., the interchain charge-bond interaction, denoted X in the literature.[16] We keep the dominant contributions that only involve one center in each chain, denoted as $X^{\perp}(\mu_1,\nu_2)$, then

$$[p_1q_1|r_1s_2]=\sum_{\mu_1\nu_2}\Psi_{p_1\mu_1}\Psi_{q_1\mu_1}\Psi_{r_1\mu_1}\Psi_{s_2\nu_2}[\mu_1\mu_1|\mu_1\nu_2] = \sum_{\mu_1\nu_2}\Psi_{p_1\mu_1}\Psi_{q_1\mu_1}\Psi_{r_1\mu_1}\Psi_{s_2\nu_2}X^{\perp}(\mu_1,\nu_2). \tag{26}$$

The X term has been found to reduce the dimerization in polyacetylene[26–28] and also has been considered by Rice and Gartstein in the context of photoinduced charge-transfer phenomena.[29] For simplicity, we assume an exponential dependence on distance $e^{-\xi r}$ for both the $t^{\perp}$ and $X^{\perp}$ terms with ξ being chosen as reciprocal of π-orbital radius ($\sim$0.7 Å):

$$t^{\perp}(\mu_1,\nu_2)=t^{\perp}e^{-\zeta z(\mu_1,\nu_2)}, \tag{27a}$$

$$X^{\perp}(\mu_1,\nu_2)=X^{\perp}e^{-\zeta z(\mu_1,\nu_2)}, \tag{27b}$$

where $z(\mu_1,\nu_2)$ is the distance between two carbon atoms. We treat the ratio $X^{\perp}/t^{\perp}$ as a variable.

We consider two limiting cases. (i) That of weak intermolecular coupling, the electronic states being localized on single chains [represented by Eqs. (25a)–(25d)]. We can consider that this corresponds to the large static disorder limit because of the disorder aspects of single chains (even though disorder is not explicitly taken into account in this work). (ii) That of strong coupling, the electronic states being then coherent.

A. Weak coupling

The ratio of singlet to triplet cross-section in the large static disorder limit is given for electron transfer (ET) as

$$\sigma^{\mathrm{ET}}_{S/T}=|\langle \mathrm{in}_1|H'|\mathrm{fi}_{1S}\rangle|^2/|\langle \mathrm{in}_1|H'|\mathrm{fi}_{1T}\rangle|^2 = \kappa\frac{(C_{1L}+C_{3L}+Z_1)(C_{1R}+C_{3R}+Z_2)}{(C'_{1L}-C'_{3L}+Z'_1)(C'_{1R}-C'_{3R}+Z'_2)}, \tag{28}$$

$$\sigma^{\mathrm{HT}}_{S/T}=|\langle \mathrm{in}_2|H'|\mathrm{fi}_{1S}\rangle|^2/|\langle \mathrm{in}_2|H'|\mathrm{fi}_{1T}\rangle|^2 = \kappa\frac{(-C_{2L}+C_{4L}+Z_3)(-C_{2R}+C_{4R}+Z_4)}{(-C'_{2L}-C'_{4L}+Z'_3)(-C'_{2R}-C'_{4R}+Z'_4)}, \tag{29}$$

where S/T denotes singlet/triplet and $\kappa=\langle \mathrm{ex}_S|\mathrm{ex}_S\rangle/\langle \mathrm{ex}_T|\mathrm{ex}_T\rangle$. The detailed expressions and the deductive procedure are given in the Appendix. The Z term represents the correlation effects from the double-excitation configuration.

C_1 represents the hopping of an electron from the LUMO (lowest unoccupied molecular orbital) of chain 2 to all virtual orbitals of chain 1 while C_2 represents the hopping of a hole from the HOMO (highest occupied molecular orbital) of chain 2 to all occupied orbitals of chain 1. Usually, the hopping integral $t^{\perp}$ is negative and $X^{\perp}$ is positive. Equation (A17) in the Appendix indicates that the renormalization effect of the X term tends to reduce $t^{\perp}$. C_3 and C_4 are pure correlation effects, that provide the distinction between singlet and triplet excitations in charge-transfer processes. The C' terms in the denominators are defined in the same way as the C terms in the numerators; the former are evaluated with the triplet exciton wavefunction and the latter with the singlet.

B. Strong coupling

For strong coupling, the electronic states are coherent combinations of localized states

$$|D_1\rangle=(|\mathrm{fi}_1\rangle+|\mathrm{fi}_2\rangle)/\sqrt{2}, \tag{30a}$$

$$|D_2\rangle=(|\mathrm{fi}_1\rangle-|\mathrm{fi}_2\rangle)/\sqrt{2}, \tag{30b}$$

$$|D_3\rangle=(|\mathrm{in}_1\rangle+|\mathrm{in}_2\rangle)/\sqrt{2}, \tag{30c}$$

$$|D_4\rangle=(|\mathrm{in}_1\rangle-|\mathrm{in}_2\rangle)/\sqrt{2}, \tag{30d}$$

(note that $\langle D_1|H'|D_4\rangle=\langle D_2|H'|D_3\rangle=0$). In the limiting case of delocalized excitations, the effects of electron transfer and hole transfer are coherently mixed, constructively for D_1 and destructively for D_2. The ratio of singlet/triplet formation cross-sections for Davydov states can then be expressed as follows.

For D_1:

$$\sigma^{D_1}_{S/T}=|\langle D_3|H'|D_{1S}\rangle|^2/|\langle D_3|H'|D_{1T}\rangle|^2=\kappa\frac{(C_{1L}-C_{2L}+C_{3L}+C_{4L}+Z_1+Z_3)(C_{1R}-C_{2R}+C_{3R}+C_{4R}+Z_2+Z_4)}{(C'_{1L}-C'_{2L}+C'_{3L}+C'_{4L}+Z'_1+Z'_3)(C'_{1R}-C'_{2R}+C'_{3R}+C'_{4R}+Z'_2+Z'_4)} \tag{31}$$

For D_2:

$$\sigma^{D_2}_{S/T}=|\langle D_4|H'|D_{2S}\rangle|^2/|\langle D_4|H'|D_{2T}\rangle|^2=\kappa\frac{(C_{1L}+C_{2L}+C_{3L}-C_{4L}+Z_1+Z_3)(C_{1R}+C_{2R}+C_{3R}-C_{4R}+Z_2+Z_4)}{(C'_{1L}+C'_{2L}+C'_{3L}-C'_{4L}+Z'_1+Z'_3)(C'_{1R}+C'_{2R}+C'_{3R}-C'_{4R}+Z'_2+Z'_4)}. \tag{32}$$

In this case, the correlation effect for the Davydov state D_1 is much more pronounced than in the disorder case, because electron and hole contributions are constructive for the correlation terms (C_3+C_4) and destructive for the mean field terms (C_1-C_2). However, for the D_2 excited state, it is constructive for the mean field terms (C_1+C_2) and destructive for the correlation terms (C_3-C_4). Thus, correlation effects are expected to be much less important for D_2 than D_1.

IV. RESULTS AND DISCUSSION

To estimate the magnitude of the effects in the weak and strong coupling limits, we have carried out numerical calcu-

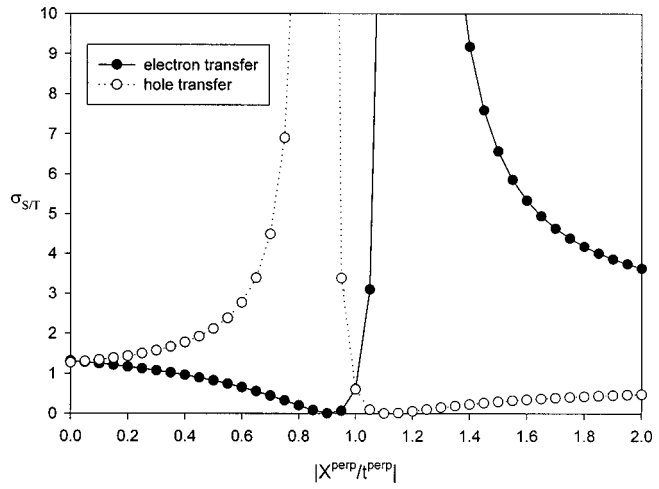

FIG. 3. Evolution of the ratio of singlet to triple exciton formation rate $\sigma_{S/T}$ for electron (closed circles) and hole (open circles) transfer as a function of $|X^{\perp}/t^{\perp}|$.

lations for two six-ring PPV oligomers interacting in a cofacial arrangement with an interchain distance of 4 Å. Figures 3 and 4 display the evolution of the ratio of the singlet to triplet cross sections as a function of $|X^{\perp}/t^{\perp}|$ for the disorder and coherent cases, respectively. For convenience, we fix $t^{\perp}=-1$ and change the value of $X^{\perp}$.

In the weak coupling limit, Fig. 3, we find that the electron transfer channel favors triplet exciton formation for $0.2<|X^{\perp}/t^{\perp}|<1$, while the hole transfer channel favors the singlet. Since there usually exist deep trap centers that inhibit electron transfer in PPV and its derivatives, holes are in most cases the majority charge carriers.[30,31]

We emphasize that the ratio becomes large only when $X^{\perp}$ is comparable to $-t^{\perp}$; this occurs for hole transfer for $|X^{\perp}/t^{\perp}|\sim 0.8$ and for electron transfer for $|X^{\perp}/t^{\perp}|\sim 1.2$. However, usually $|X^{\perp}/t^{\perp}|\ll 0.8$; in this case, there is not much difference between the formation probabilities of singlet and triplet excitons in the weak coupling (strong disorder) limit.

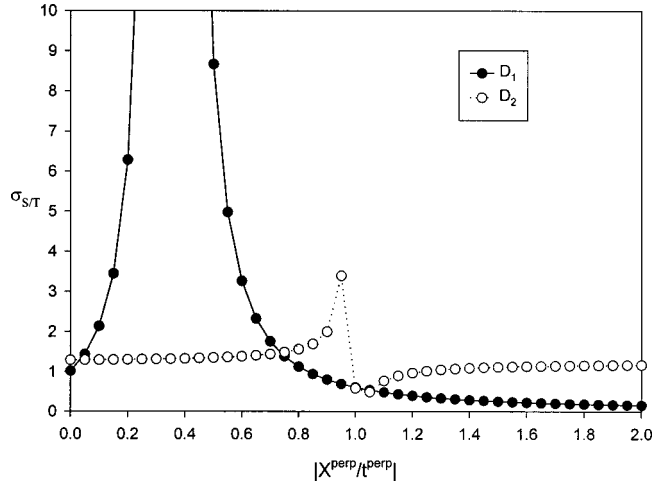

FIG. 4. Evolution of the ratio of singlet to triplet exciton formation rate $\sigma_{S/T}$ for D_1 (closed circles) and D_2 (open circles) as a function of $|X^{\perp}/t^{\perp}|$.

For $X^{\perp}=0$, the singlet to triplet ratio is around 1.3, then $\eta_2=30\%$, slightly larger than the statistical limit of 25%. This is due to the difference in the CI coefficients for the singlet and triplet excitons. The contribution from the HOMO-LUMO excitation configuration for the singlet exciton is larger than that for the triplet exciton. It fact, the magnitude of the terms such as

$$\sum_{\mu\nu\sigma} L_{\mu}^{\text{singlet}} U_{\nu} X_{\sigma} \langle \cdots \rangle$$

in the Appendix [Eq. (A12)] are slightly larger than that of the terms

$$\sum_{\mu\nu\sigma} L_{\mu}^{\text{triplet}} U_{\nu} X_{\sigma} \langle \cdots \rangle,$$

then $\sigma_{S/T}>1$. The lowest molecular charge transfer state can be mostly represented by the frontier orbitals, even within the CCSD-EOM description.

In the case of full coherence, Fig. 4, the two Davydov states have different behaviors as $|X^{\perp}/t^{\perp}|$ increases. For the optically active state $|D_1\rangle$, there occurs a resonance for $|X^{\perp}/t^{\perp}|$ in the range 0.1 to 0.6. This is the consequence of an amplified correlation effect. For the optically forbidden state $|D_2\rangle$, the ratio is around 1.3 in this range and the singlet is slightly favorable.

To explain this qualitatively, we can simplify Eqs. (A16a)–(A16d) and (A21a)–(A21d) in the Appendix as

$$C_1 \sim \alpha_1 t^{\perp} + \beta_1 X^{\perp}, \tag{33a}$$

$$C_2 \sim \alpha_2 t^{\perp} + \beta_2 X^{\perp}, \tag{33b}$$

$$C_3 \sim \gamma_1 X^{\perp}, \tag{33c}$$

$$C_4 \sim \gamma_2 X^{\perp} \tag{33d}$$

(note that $t^{\perp}\langle 0, X^{\perp}\rangle 0$), where α represents the effect of hopping of an electron or hole, β represents the renormalization effect, and γ represents the pure correlation effects. Then, Eqs. (28), (29), (31), and (32) can be written as

$$\sigma_{S/T}^{\text{ET}} \sim \left(\frac{-\alpha_1^S + (\beta_1^S + \gamma_1^S)|X^{\perp}/t^{\perp}|}{-\alpha_1^T + (\beta_1^T - \gamma_1^T)|X^{\perp}/t^{\perp}|} \right)^2, \tag{34a}$$

$$\sigma_{S/T}^{\text{HT}} \sim \left(\frac{\alpha_2^S + (-\beta_2^S + \gamma_2^S)|X^{\perp}/t^{\perp}|}{\alpha_2^T + (-\beta_2^T - \gamma_2^T)|X^{\perp}/t^{\perp}|} \right)^2, \tag{34b}$$

$$\sigma_{S/T}^{D_1} \sim \left(\frac{\alpha_2^S - \alpha_1^S + (\beta_1^S - \beta_2^S + \gamma_1^S + \gamma_2^S)|X^{\perp}/t^{\perp}|}{\alpha_2^T - \alpha_1^T + (\beta_1^T - \beta_2^T - \gamma_1^T - \gamma_2^T)|X^{\perp}/t^{\perp}|} \right)^2, \tag{34c}$$

$$\sigma_{S/T}^{D_2} \sim \left(\frac{-\alpha_1^S - \alpha_2^S + (\beta_1^S + \beta_2^S + \gamma_1^S - \gamma_2^S)|X^{\perp}/t^{\perp}|}{-\alpha_1^T - \alpha_2^T + (\beta_1^T + \beta_2^T - \gamma_1^T + \gamma_2^T)|X^{\perp}/t^{\perp}|} \right)^2. \tag{34d}$$

For ET, when $|X^{\perp}/t^{\perp}| \to \alpha_1^T/(\beta_1^T - \gamma_1^T)$, $\sigma_{S/T}^{\text{ET}}$ reaches a maximum. For HT, $\sigma_{S/T}^{\text{HT}}$ reaches a maximum when $|X^{\perp}/t^{\perp}| \to \alpha_2^T/(\beta_2^T + \gamma_2^T)$. In our model for PPV6, $\alpha_1^T/(\beta_1^T - \gamma_1^T)$

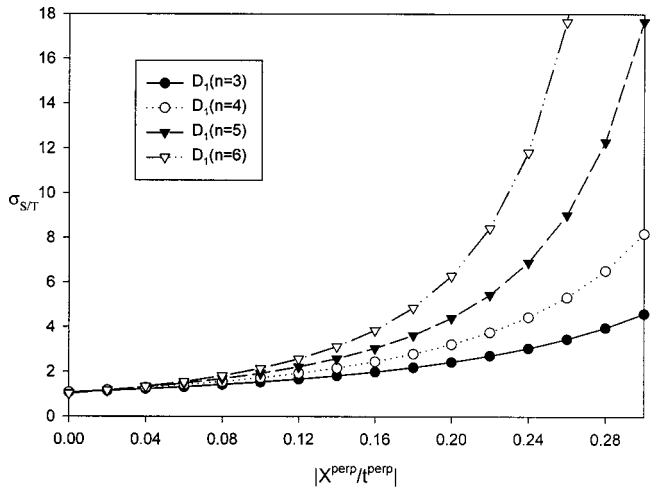

FIG. 5. Evolution for four PPV oligomers of various length (n being the number of phenylene rings) of the ratio of singlet to triplet exciton formation rate $\sigma_{S/T}$ for D_1 as a function of $|X^{\perp}/t^{\perp}|$.

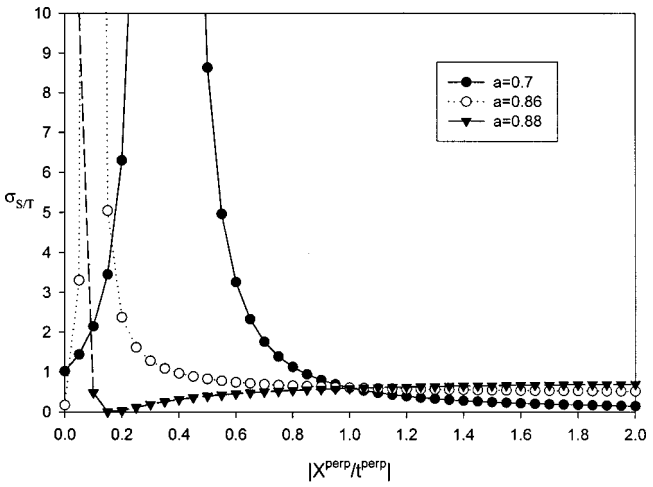

FIG. 6. Evolution of the ratio of singlet to triplet exciton formation rate $\sigma_{S/T}$ for D_1' with coefficient $a=0.7$ (closed circles), 0.86 (opened circles), and 0.88 (closed triangles) appearing in Eqs. (35a)–(35d) as a function of $|X^{\perp}/t^{\perp}|$.

~ 1.2 and $\alpha_2^T/\beta_2^T+\gamma_2^T\sim 0.8$. We can conclude that the magnitude of α is the same as that of β, but is significantly larger than γ.

For D_1, $\sigma_{S/T}^{D_1}$ reaches a maximum when

$$|X^{\perp}/t^{\perp}|\rightarrow \frac{\alpha_2^T-\alpha_1^T}{\beta_2^T-\beta_1^T+\gamma_1^T+\gamma_2^T}.$$

We find that the hopping effect α and the renormalization effect β are destructive, while the correlation effects γ are constructive. As a consequence, the magnitude of $(\alpha_2^T-\alpha_1^T)$ and $(\beta_2^T-\beta_1^T)$ is the same as that of $(\gamma_1^T+\gamma_2^T)$. The pure correlation effect γ takes a very important role. In our model,

$$\frac{\alpha_2^T-\alpha_1^T}{\beta_2^T-\beta_1^T+\gamma_1^T+\gamma_2^T}\sim 0.4.$$

For D_2, we find that the hopping effect α and the renormalization effect β are destructive, while the correlation effects γ are constructive. Then, $(\alpha_2^T+\alpha_1^T)\gg(\gamma_1^T-\gamma_2^T)$ and $(\alpha_2^T+\alpha_1^T)\gg(\gamma_1^T-\gamma_2^T)$. It leads to $\sigma_{S/T}^{D_2}\sim 1$.

In the experiments of Cao *et al.*,[8] electron-transport materials are blended with PPV to ensure balanced injections of holes and electrons. This is expected to improve the coherence between electrons and holes, so that the scenario associated with the limiting case of Fig. 4 becomes applicable. In this case, $|X^{\perp}/t^{\perp}|=0.13$ gives $\sigma_{S/T}\sim 3$, namely, $\eta_2=50\%$. Figure 5 shows $\sigma_{S/T}$ for D_1 obtained with PPVn, with n the number of aromatic rings. We find that $\sigma_{S/T}$ in the resonance range increases with the number of phenylene rings. The reason is that the increase of the length of the PPV chain results in the increase of the pure correlation effects γ. In Eq. (34c), the denominator decreases and the numerator increases; thus, $\sigma_{S/T}^{D_1}$ increases in the resonance range.

To study the situation intermediate between the weak coupling limit and the strong coupling limit, we modify the electronic states, Eqs. (30a)–(30d), as

$$|D_1'\rangle=a|\mathrm{fi}_1\rangle+\sqrt{1-a^2}|\mathrm{fi}_2\rangle, \tag{35a}$$

$$|D_2'\rangle=\sqrt{1-a^2}|\mathrm{fi}_1\rangle-a|\mathrm{fi}_2\rangle, \tag{35b}$$

$$|D_3'\rangle=a|\mathrm{in}_1\rangle+\sqrt{1-a^2}|\mathrm{in}_2\rangle, \tag{35c}$$

$$|D_4'\rangle=\sqrt{1-a^2}|\mathrm{in}_1\rangle-a|\mathrm{in}_2\rangle. \tag{35d}$$

When $a=0$ or 1, it corresponds to the weak coupling limit; when $a=0.7$, it is the strong coupling limit. Then, Eq. (34c) becomes

$$\sigma_{S/T}^{D_1'}\sim\left(\frac{\theta\alpha_2^S-\alpha_1^S+(\beta_1^S-\theta\beta_2^S+\gamma_1^S+\theta\gamma_2^S)|X^{\perp}/t^{\perp}|}{\theta\alpha_2^T-\alpha_1^T+(\beta_1^T-\theta\beta_2^T-\gamma_1^T-\theta\gamma_2^T)|X^{\perp}/t^{\perp}|}\right)^2, \tag{36}$$

where $\theta=2a\sqrt{1-a^2}$. When

$$|X^{\perp}/t^{\perp}|\rightarrow\frac{\theta\alpha_2^T-\alpha_1^T}{\theta\beta_2^T-\beta_1^T+\gamma_1^T+\theta\gamma_2^T},$$

$\sigma_{S/T}^{D_1'}$ reaches a maximum. Figures 6 and 7 display the evolution of the ratio of the singlet to triplet cross sections as a function of $|X^{\perp}/t^{\perp}|$ for D_1' with various coefficients a in the range 0.7 to 1. There are four situations.

(1) $\theta\alpha_2^T-\alpha_1^T>0, \theta\beta_2^T-\beta_1^T+\gamma_1^T+\theta\gamma_2^T>0$. As the values of coefficient a increase, θ decreases and the maximum of $\sigma_{S/T}^{D_1'}$ moves toward the left, see the cases $a=0.7$ and $a=0.86$ in Fig. 6: the resonance range moves toward the left and becomes narrower with the increase of a.

(2) $\theta\alpha_2^T-\alpha_1^T\approx 0, \theta\beta_2^T-\beta_1^T+\gamma_1^T+\theta\gamma_2^T>0$. The maximum of $\sigma_{S/T}^{D_1'}$ is around zero, see the case $a=0.88$ in Fig. 6; the resonance range is very narrow.

(3) $\theta\alpha_2^T-\alpha_1^T<0, \theta\beta_2^T-\beta_1^T+\gamma_1^T+\theta\gamma_2^T>0$. $\sigma_{S/T}^{D_1'}$ remains small and there is no resonance range (we can imagine that

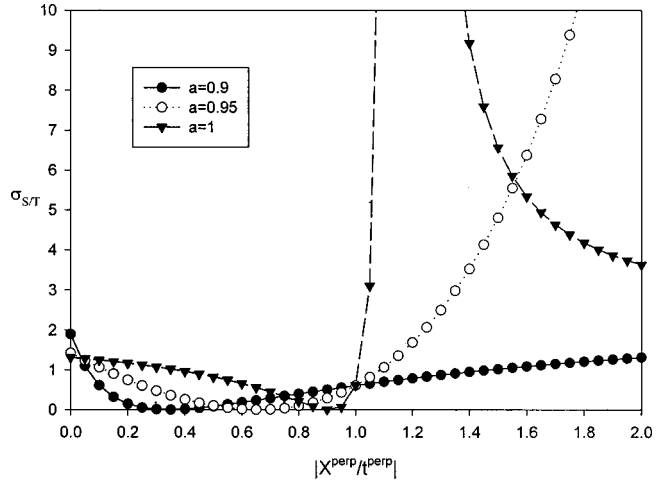

FIG. 7. Evolution of the ratio of singlet to triplet exciton formation rate $\sigma_{S/T}$ for D_1' with coefficient $a=0.9$ (closed circles), 0.95 (opened circles), and 0.1 (closed triangles) appearing in Eqs. (35a)–(35d) as a function of $|X^{\perp}/t^{\perp}|$.

the resonance range actually moves into the negative region of $|X^{\perp}/t^{\perp}|$ as a increases), see the case $a=0.9$ in Fig. 7.

(4) $\theta\alpha_2^T-\alpha_1^T<0, \theta\beta_2^T-\beta_1^T+\gamma_1^T+\theta\gamma_2^T<0$. The maximum of $\sigma_{S/T}^{D_1'}$ moves toward the left from ∞ to $a=1$, see the cases $a=0.95$ and $a=1$ in Fig. 7.

The evolution of $\sigma_{S/T}^{D_1'}$ with a in the range 0 to 0.7 is similar. Usually $|X^{\perp}/t^{\perp}|$ is very small, so we do not consider the situations depicted in Fig. 7 but those in Fig. 6. Since $|X^{\perp}/t^{\perp}|$ is determined by the property of the polymer, in the experiment, the electron or hole transfer materials can be blended to change coefficient a to make the resonance range coincide with $|X^{\perp}/t^{\perp}|$. It can make $\sigma_{S/T}$ as big as possible.

In our model, we find that σ is only affected by the lowest singlet and triplet excitation states. The other higher excitation states do not exert any influence. The results are illustrated in Fig. 8. Kobrak and Bittner indicated that both σ_S and σ_T depend on the relative energies of the lowest singlet and triplet states.[14] In order to find out the dependence of the

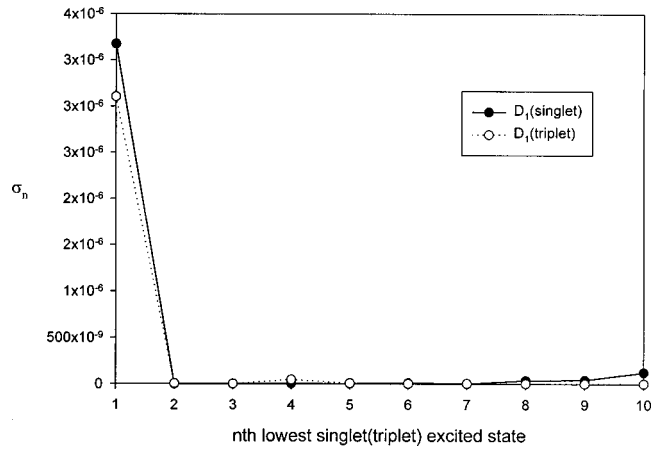

FIG. 8. Cross section σ_n for nth lowest singlet (closed circles) and triplet (open circles) excited states for D_1.

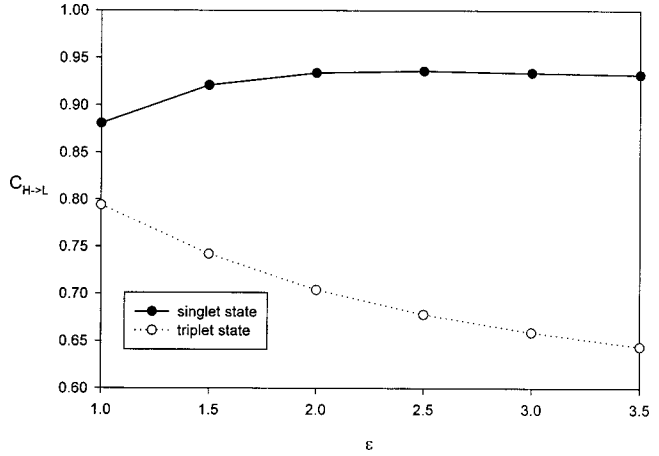

FIG. 9. Evolution of coefficient $C_{H\to L}$ in Eq. (37) for singlet (closed circles) and triplet (open circles) states as a function of the dielectric constant ε appearing in the Ohno-Klopman potential [Eq. (21)].

electroluminescence quantum yield η_2 on the singlet and triplet state energies, we vary the value of the dielectric constant ε in the Ohno-Klopman potential [Eq. (21)]: a larger ε induces a greater exchange energy so that the triplet state becomes more stabilized. For the sake of simplicity, we performed the calculations on the shorter oligomer PPV3.

The lowest excited state can be expressed as

$$|\mathrm{ex}\rangle = C_{H\to L}|\mathrm{HOMO}\to\mathrm{LUMO}\rangle + \text{other excitation configurations.} \quad (37)$$

We illustrate the evolution of coefficient $C_{H\to L}$ for singlet and triplet states as a function of the dielectric constant ε appearing in the Ohno-Klopman potential [Eq. (21)] in Fig. 9. It is found that $C_{H\to L}$ increases slightly for the singlet state as ε increases, while it decreases significantly for the triplet state. This is due to the difference in character between the singlet and triplet states, the former being ionic

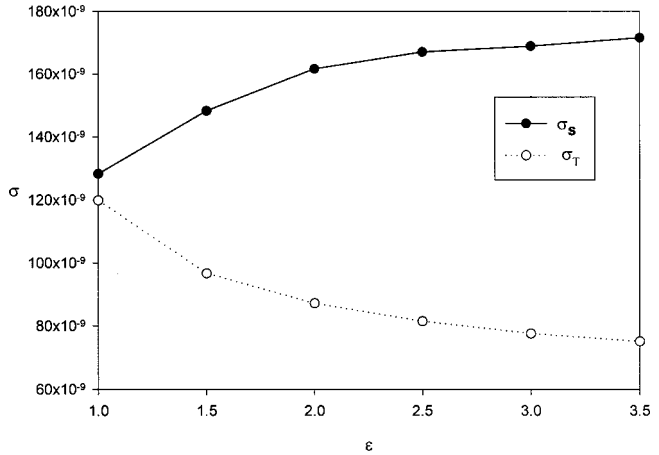

FIG. 10. Evolution for PPV3 of the singlet cross section σ_S (closed circles) and the triplet cross section σ_T (open circles) for D_1 with $|X^{\perp}/t^{\perp}|=0$ as a function of the dielectric constant appearing in the Ohno-Klopman potential [Eq. (21)].

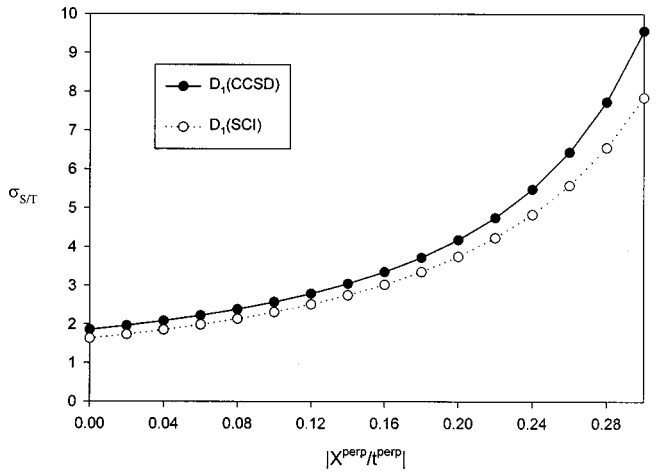

FIG. 11. Evolution for PPV3 of the ratio of singlet to triplet exciton formation rate $\sigma_{S/T}$ for D_1 obtained by CCSD (closed circles) and by SCI (open circles) for $\varepsilon=2$ as a function of $|X^{\perp}/t^{\perp}|$.

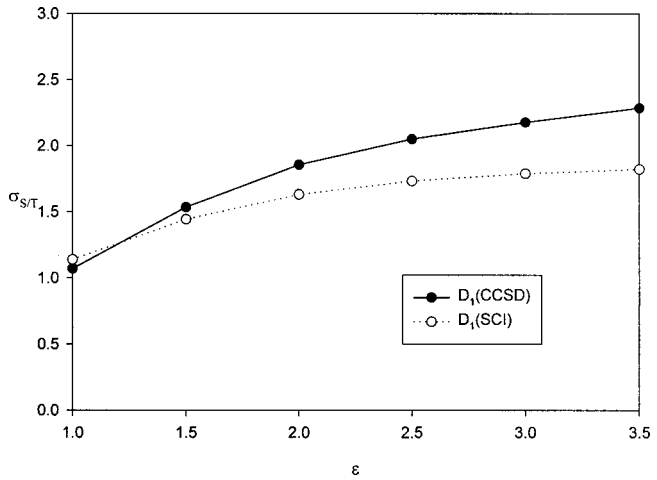

FIG. 12. Evolution of the ratio of singlet to triple exciton formation rate $\sigma_{S/T}$ for D_1 with $|X^{\perp}/t^{\perp}|=0$ obtained by CCSD (closed circles) and by SCI (open circles) as a function of the dielectric constant ε appearing in the Ohno-Klopman potential [Eq. (21)].

while the latter is covalent.[32] It results in the increase of the singlet cross-section σ_S and the decrease of the triplet cross section σ_T as the value of ε increases. This is illustrated in Fig. 10, where we fix $|X^{\perp}/t^{\perp}|=0$ such that the contribution of on-chain correlation to the formation rate is clearly demonstrated.

When $\varepsilon=1$, our results are similar to those we obtained in our previous work, where a single CI approach is applied. When increasing the value of ε, the value of $\sigma_{S/T}$ becomes larger than that obtained by a single CI treatment. The results are illustrated in Fig. 11, where we set $\varepsilon=2$. We illustrate the evolution of the ratio of singlet to triplet exciton formation rate $\sigma_{S/T}$ as a function of the dielectric constant ε in Fig. 12, where we take $|X^{\perp}/t^{\perp}|=0$ as an example. This clearly indicates the correlation effects coming from excitation double configurations cannot be neglected.

To summarize, we have calculated the formation cross-section ratio of singlet to triplet excitons occurring in PPV through interchain charge-transfer (CT) processes. Wohlgenannt *et al.* indicated that the CT process is an intermediate step in which a metastable encounter complex (EC) is formed.[10] $|\mathrm{EC}\rangle$ is a superposition of the initial states $|\mathrm{in}\rangle$ and final states $|\mathrm{fi}\rangle$. Since the states $|n\rangle$ and $|p\rangle$ are ionic, $|\mathrm{EC}\rangle$ is ionic. Note that the singlet states are ionic while the triplet states are covalent. This leads to the conclusion that $\sigma_S > \sigma_T$. We found that correlation effects of bond-charge type are an important factor differentiating singlet from triplet exciton formation rates. The correlation effects are very pronounced for the optically allowed Davydov exciton state, where even a small bond-charge interaction can bring a large difference in singlet and triplet formation cross sections. The ratio between the electroluminescence and photoluminescence quantum yields generally exceeds the 25% spin degeneracy statistical limit. Based on the different nature of the singlet and triplet excitons, the rates of formation of the singlet and triplet excitons strongly depends on the electron-electron potential.

ACKNOWLEDGMENTS

The work was partly supported by the Belgian Federal Services for Scientific, Technical, and Cultural Affairs (Inter-University Attraction Pole, Program No. PAI 4/11), the Belgian National Fund for Scientific Research (FNRS/FREC), and the U.S. National Science Foundation (Grant No. CHE-0078819).

APPENDIX: THEORETICAL DETAILS

1. $\bar{H}_{\sigma\rho}$ matrix elements for the positively charged state

They are evaluated as

$$\bar{H}_{SS}=\langle l^{+}\bar{H}k\rangle=(E_{\mathrm{CC}}-\varepsilon_k)\,\delta_{lk}+\sum_{ai}\langle ki\|al\rangle t_i^a+\sum_{\substack{i\\a>b}}\langle ik\|ab\rangle t_{li}^{ab}+\sum_{abi}\langle ki\|ab\rangle t_i^a t_l^b, \tag{A1}$$

$$\bar{H}_{SD}=\langle k^{+}Hc^{+}ml\rangle=\langle lm\|ck\rangle+\sum_{a}\langle ml\|ac\rangle t_k^a+\delta_{kl}\sum_{ia}\langle im\|ac\rangle t_i^a-\delta_{km}\sum_{ia}\langle il\|ac\rangle t_i^a, \tag{A2}$$

$$\bar{H}_{DS}=\langle l^{+}m^{+}cHk\rangle=\delta_{kl}\gamma(c,m)-\delta_{km}\gamma(c,l)+\chi(c,k,l,m), \tag{A3}$$

where

$$\gamma(c,m)=(\varepsilon_c-\varepsilon_m)t_m^c+\sum_{ai}\langle ic\|am\rangle t_i^a+\sum_{\substack{i\\a>b}}\langle li\|ab\rangle t_{mi}^{ab}+\sum_{\substack{a\\i>j}}\langle ji\|am\rangle t_{ij}^{ac}+\sum_{abi}\langle ic\|ab\rangle t_i^a t_m^b+\sum_{aij}\langle ji\|am\rangle t_i^a t_j^c$$

$$+\sum_{abij}\langle ji\|ab\rangle t_i^a t_{jm}^{cb}+\sum_{\substack{ab\\i>j}}\langle ji\|ab\rangle t_m^a t_{ij}^{cb}+\sum_{\substack{ij\\a>b}}\langle ji\|ab\rangle t_i^c t_{mj}^{ab}+\sum_{abij}\langle ji\|ab\rangle t_m^a t_j^b t_i^c,$$

$$\chi(c,k,l,m)=\langle ck\|lm\rangle+\sum_i\langle ki\|lm\rangle t_i^c+\sum_a\langle ck\|am\rangle t_l^a-\sum_a\langle ck\|al\rangle t_m^a+\sum_{ai}\langle ik\|am\rangle t_{il}^{ac}-\sum_{ai}\langle ik\|al\rangle t_{im}^{ac}+\sum_{a>b}\langle ck\|ab\rangle t_{lm}^{ab}$$

$$+\sum_{ab}\langle ck\|ab\rangle t_l^a t_m^b+\sum_{ai}\langle ki\|am\rangle t_l^a t_i^c-\sum_{ai}\langle ki\|al\rangle t_m^a t_i^c+\sum_{abi}\langle ik\|ab\rangle t_m^a t_{il}^{cb}-\sum_{abi}\langle ik\|ab\rangle t_l^a t_{im}^{cb}$$

$$+\sum_{abi}\langle ki\|ab\rangle t_i^a t_{lm}^{bc}+\sum_{\substack{i\\a>b}}\langle ki\|ab\rangle t_i^c t_{lm}^{ab}+\sum_{abi}\langle ki\|ab\rangle t_l^a t_m^b t_i^c,$$

$$\bar{H}_{DD}=\langle n^+ o^+ eHd^+ ml\rangle$$

$$=\delta_{ed}\delta_{nl}\delta_{om}(E_{\mathrm{CC}}-\varepsilon_n-\varepsilon_o+\varepsilon_e)+\delta_{nl}\delta_{om}\xi(e,d)+\delta_{ed}\delta_{om}\sigma(n,l)-\delta_{ed}\delta_{ol}\sigma(n,m)-\delta_{ed}\delta_{nm}\sigma(o,l)+\delta_{ed}\delta_{nl}\sigma(o,m)$$

$$+\delta_{om}\beta(d,n,l,e)-\delta_{ol}\beta(d,n,m,e)-\delta_{nm}\beta(d,o,l,e)+\delta_{nl}\beta(d,o,m,e)+\delta_{ed}\alpha(o,n,m,l)+\sum_a\langle ml\|ad\rangle t_{no}^{ae},\qquad\text{(A4)}$$

where

$$\sigma(n,l)=\sum_{ia}\langle li\|an\rangle t_i^a+\sum_{\substack{a\\i>j}}\langle ji\|ad\rangle t_{ij}^{ae}+\sum_{abi}\langle li\|ab\rangle t_i^a t_n^b,$$

$$\xi(e,d)=\sum_{ai}\langle ie\|ad\rangle t_i^a+\sum_{\substack{i\\a>b}}\langle li\|ab\rangle t_{in}^{ab}-\sum_{aij}\langle ij\|ad\rangle t_i^a t_j^e,$$

$$\alpha(o,n,m,l)=\langle ml\|on\rangle+\sum_a\langle ml\|an\rangle t_o^a-\sum_a\langle ml\|ao\rangle t_n^a+\sum_{a>b}\langle lm\|ab\rangle t_{no}^{ab}+\sum_{ab}\langle ml\|ab\rangle t_o^a t_n^b,$$

$$\beta(d,n,l,e)=\langle le\|dn\rangle+\sum_i\langle li\|nd\rangle t_i^e+\sum_a\langle el\|ad\rangle t_n^a+\sum_{ai}\langle il\|ad\rangle t_{in}^{ac}+\sum_{ai}\langle li\|ad\rangle t_n^a t_i^e.$$

It should be noted that the excitation configuration is not a spin-symmetry adapted basis. The z component is either $\frac{1}{2}$ or $-\frac{1}{2}$. For $S=\frac{1}{2}$, we need to make the proper linear combination of the basis. There are four types (out of six) of basis for $S=\frac{1}{2}$ and $S_z=\frac{1}{2}(|\sigma\rangle_\uparrow)$:

$$\text{(i)}\quad |m_\beta\rangle,\qquad\text{(A5a)}$$

$$\text{(ii)}\quad |c_\alpha^+ m_\alpha m_\beta\rangle,\qquad\text{(A5b)}$$

$$\text{(iii)}\quad (-2|c_\beta^+ m_\beta l_\beta\rangle+|c_\alpha^+ m_\alpha l_\beta\rangle+|c_\alpha^+ m_\beta l_\alpha\rangle)/\sqrt{6},\qquad\text{(A5c)}$$

$$\text{(iv)}\quad (|c_\alpha^+ m_\alpha l_\beta\rangle-|c_\alpha^+ m_\beta l_\alpha\rangle)/\sqrt{2}.\qquad\text{(A5d)}$$

The $S=\frac{1}{2}$ and $S_z=-\frac{1}{2}$ spin basis $|\sigma\rangle_\downarrow$ is obtained by exchanging the indices α and β of eigenstates $|\sigma\rangle_\uparrow$ in Eqs. (A5a)–(A5d).

2. $\bar{H}_{\mu\nu}$ matrix elements for the negatively charged state

They are evaluated as

$$\bar{H}_{SS}=\langle c\bar{H}d^+\rangle=\delta_{cd}(E_{\mathrm{CC}}+\varepsilon_c)+\sum_{ai}\langle ic\|ad\rangle t_i^a+\sum_{\substack{a\\i>j}}\langle ij\|ad\rangle t_{ij}^{ca}-\sum_{ija}\langle ij\|ad\rangle t_i^a t_j^c,\qquad\text{(A6)}$$

$$\bar{H}_{SD}=\langle c\bar{H}e^{+}d^{+}k\rangle=\langle ck\|de\rangle+\sum_{i}\langle ki\|ed\rangle t_i^c+\delta_{cd}\sum_{ia}\langle ki\|ae\rangle t_i^a-\delta_{ce}\sum_{ia}\langle ki\|ad\rangle t_i^a, \tag{A7}$$

$$\bar{H}_{DS}=\langle k^{+}de\bar{H}c^{+}\rangle=\delta_{cd}\gamma'(k,e)-\delta_{ce}\gamma'(k,d)+\chi'(e,d,c,k), \tag{A8}$$

where

$$\gamma'(k,e)=(\varepsilon_k-\varepsilon_e)t_k^e-\sum_{ai}\langle ie\|ak\rangle t_i^a-\sum_{\substack{i\\a>b}}\langle ie\|ab\rangle t_{ik}^{ab}+\sum_{\substack{a\\i>j}}\langle ij\|ak\rangle t_{ij}^{ae}-\sum_{abi}\langle ie\|ab\rangle t_i^a t_k^b+\sum_{aij}\langle ij\|ak\rangle t_i^a t_j^e$$

$$+\sum_{abij}\langle ij\|ab\rangle t_i^a t_{jk}^{eb}+\sum_{\substack{ab\\i>j}}\langle ij\|ab\rangle t_k^a t_{ij}^{eb}+\sum_{\substack{ij\\a>b}}\langle ij\|ab\rangle t_i^e t_{jk}^{ab}-\sum_{abij}\langle ij\|ab\rangle t_i^b t_j^e t_k^a,$$

$$\xi'(e,d,c,k)=\langle ed\|ck\rangle+\sum_{i}\langle ie\|ck\rangle t_i^d-\sum_{i}\langle id\|ck\rangle t_i^e+\sum_{a}\langle de\|ac\rangle t_k^a+\sum_{ai}\langle ie\|ac\rangle t_{ik}^{ad}-\sum_{ai}\langle id\|ac\rangle t_{ik}^{ae}+\sum_{i>j}\langle ij\|kc\rangle t_{ij}^{de}$$

$$-\sum_{ij}\langle ij\|ck\rangle t_i^d t_j^e+\sum_{ai}\langle id\|ac\rangle t_k^a t_i^e-\sum_{ai}\langle ie\|ac\rangle t_k^a t_i^d+\sum_{ija}\langle ij\|ac\rangle t_i^a t_{jk}^{de}-\sum_{ija}\langle ij\|ac\rangle t_i^e t_{jk}^{da}+\sum_{ija}\langle ij\|ac\rangle t_i^d t_{jk}^{ea}$$

$$+\sum_{\substack{a\\i>j}}\langle ij\|ac\rangle t_k^a t_{ij}^{de}-\sum_{ija}\langle ij\|ac\rangle t_i^e t_j^d t_k^a,$$

$$\bar{H}_{DD}=\langle k^{+}cd\bar{H}f^{+}e^{+}l\rangle=\delta_{kl}\delta_{ce}\delta_{df}(E_{\mathrm{CC}}+\varepsilon_d+\varepsilon_c-\varepsilon_k)-\sum_{i}\langle li\|fe\rangle t_{ik}^{cd}+\delta_{kl}\alpha'(d,c,f,e)+\delta_{ce}\delta_{df}\xi'(k,l)+\delta_{kl}\delta_{ce}\sigma'(d,f)$$

$$-\delta_{kl}\delta_{cf}\sigma'(d,e)-\delta_{kl}\delta_{de}\sigma'(c,f)+\delta_{kl}\delta_{df}\sigma'(c,e), \tag{A9}$$

where

$$\sigma'(d,f)=\sum_{ia}\langle id\|af\rangle t_i^a+\sum_{\substack{a\\i>j}}\langle ij\|af\rangle t_{ij}^{da}-\sum_{ija}\langle ij\|af\rangle t_i^a t_j^d,$$

$$\xi'(k,l)=\sum_{ai}\langle li\|ak\rangle t_i^a+\sum_{\substack{i\\a>b}}\langle li\|ab\rangle t_{ik}^{ab}+\sum_{abi}\langle li\|ab\rangle t_i^a t_k^b,$$

$$\alpha'(d,c,f,e)=\langle dc\|fe\rangle+\sum_{i}\langle ci\|fe\rangle t_i^d-\sum_{i}\langle di\|fe\rangle t_i^c-\sum_{i>j}\langle ij\|fe\rangle t_{ij}^{cd}-\sum_{ij}\langle ij\|fe\rangle t_i^c t_j^d,$$

$$\beta'(l,d,f,k)=\langle ld\|fk\rangle-\sum_{a}\langle ld\|af\rangle t_k^a+\sum_{i}\langle li\|kf\rangle t_i^d+\sum_{ai}\langle li\|af\rangle t_{ik}^{da}+\sum_{ai}\langle li\|af\rangle t_k^a t_i^d.$$

The four types of spin symmetry adapted basis for $S=\frac{1}{2}$ and $S_z=\frac{1}{2}(|\nu\rangle_{\uparrow})$ are

$$\text{(i)}\quad |e_\alpha\rangle, \tag{A10a}$$

$$\text{(ii)}\quad |e_\alpha^{+}e_\beta^{+}k_\beta\rangle, \tag{A10b}$$

$$\text{(iii)}\quad (-2|e_\alpha^{+}d_\alpha^{+}k_\alpha\rangle+|e_\alpha^{+}d_\beta^{+}k_\beta\rangle+|e_\beta^{+}d_\alpha^{+}k_\beta\rangle)/\sqrt{6}, \tag{A10c}$$

$$\text{(iv)}\quad (|e_\alpha^{+}d_\beta^{+}k_\beta\rangle-|e_\beta^{+}d_\alpha^{+}k_\beta\rangle)/\sqrt{2}. \tag{A10d}$$

The $S=\frac{1}{2}$ and $S_z=-\frac{1}{2}$ basis $(|\nu\rangle_{\downarrow})$ are obtained by exchanging the indices α and β of $|\nu\rangle_{\uparrow}$ in Eqs. (A10a)–(A10d).

3. The deductive procedure for $\sigma_{S/T}^{ET}$

The ratio of singlet to triplet cross-section in the large static disorder limit is given for electron transfer (ET) as

$$\sigma_{S/T}^{\mathrm{ET}}=|\langle \mathrm{in}_1|H'|\mathrm{fi}_{1S}\rangle|^2/|\langle \mathrm{in}_1|H'|\mathrm{fi}_{1T}\rangle|^2=\frac{\langle \mathrm{fi}_{1S}|H'|\mathrm{in}_1\rangle\langle \mathrm{in}_1|H'|\mathrm{fi}_{1S}\rangle}{\langle \mathrm{fi}_{1S}|\mathrm{fi}_{1S}\rangle\langle \mathrm{in}_1|\mathrm{in}_1\rangle}\Big/\frac{\langle \mathrm{fi}_{1T}|H'|\mathrm{in}_1\rangle\langle \mathrm{in}_1|H'|\mathrm{fi}_{1T}\rangle}{\langle \mathrm{fi}_{1T}|\mathrm{fi}_{1T}\rangle\langle \mathrm{in}_1|\mathrm{in}_1\rangle}, \tag{A11}$$

where S/T denotes singlet/triplet. Inserting Eqs. (12a), (12b), (17), and (25) into Eq. (A11), we obtain

$$\langle \mathrm{fi}_1|H'|\mathrm{in}_1\rangle=\frac{1}{\sqrt{2}}\sum_{\mu_1\nu_2\sigma_1} L_{\mu_1}U_{\nu_{2\uparrow}}X_{\sigma_{1\uparrow}}\langle \mu_1^+(1+\Lambda)\overline{H}'\nu_{2\uparrow}\sigma_{1\uparrow}\rangle \pm L_{\mu_1}U_{\nu_{2\downarrow}}X_{\sigma_{1\downarrow}}\langle \mu_1^+(1+\Lambda)\overline{H}'\nu_{2\downarrow}\sigma_{1\gamma}\rangle, \tag{A12}$$

$$\langle \mathrm{in}_1|H'|\mathrm{fi}_1\rangle=\frac{1}{\sqrt{2}}\sum_{\mu_1\nu_2\sigma} Y_{\sigma_{1\uparrow}}V_{\nu_{2\uparrow}}R_{\mu_1}\langle \sigma_{1\uparrow}^+\nu_{2\uparrow}^+\overline{H}'\mu_1\rangle \pm Y_{\sigma_{1\downarrow}}V_{\nu_{2\downarrow}}R_{\mu_1}\langle \sigma_{1\downarrow}^+\nu_{2\downarrow}^+\overline{H}'\mu_1\rangle, \tag{A13}$$

where $\overline{H}'=\exp(-T_1-T_2)H'\exp(T_1+T_2)$ and $+/-$ refer to singlet/triplet.

By inserting $|\sigma_{\uparrow(\downarrow)}\rangle=\{m_{\alpha(\beta)},\text{double configuration}\}$, $|\nu_{\uparrow(\downarrow)}\rangle=\{e_{\alpha(\beta)}^+,\text{double configuration}\}$, and $|\mu\rangle=\{(d_\alpha^+ l_\alpha+d_\beta^+ l_\beta)/\sqrt{2},\text{double configuration}\}$ into Eqs. (A12) and (A13), we obtain

$$\langle \mathrm{fi}_1|H'|\mathrm{in}_1\rangle=C_{1L}\pm C_{3L}+Z_1, \tag{A14}$$

$$\langle \mathrm{in}_1|H'|\mathrm{fi}_1\rangle=C_{1R}\pm C_{3R}+Z_2. \tag{A15}$$

The Z term represents the correlation effects from the double excitation configuration. These are of a very complex form that we do not write down explicitly here. The C terms are defined as

$$C_{1L}=\sum_{m_1e_2d_1} X_{m_1}U_{e_2}L_{d_1m_1}(f_{d_1e_2}+([i_1a_1|d_1e_2]+[i_2a_2|d_1e_2])t_i^a-[i_1a_1|j_1e_2]t_{i_\beta j_\alpha}^{a_\beta d_\alpha}), \tag{A16a}$$

$$C_{1R}=\sum_{m_1e_2d_1} Y_{m_1}V_{e_2}R_{d_1m_1}(f_{d_1c_2}+([i_1a_1|d_1e_2]+[i_2a_2|d_1e_2])t_i^a-[i_2a_2|j_2d_1]t_{i_\beta j_\alpha}^{a_\beta e_\alpha}), \tag{A16b}$$

$$C_{3L}=\sum_{m_1e_2d_1l_1} X_{m_1}U_{e_2}L_{d_1l_1}([l_1d_1|m_1e_2]-[i_1l_1|m_1e_2]t_i^d+[d_1a_1|m_1e_2]t_l^a-[i_1a_1|m_1e_2]t_{i_\alpha l_\alpha}^{d_\alpha a_\alpha}), \tag{A16c}$$

$$C_{3R}=\sum_{m_1e_2d_1l_1} Y_{m_1}V_{e_2}L_{d_1l_1}([l_1d_1|m_1e_2]-[i_2m_1|l_1d_1]t_i^e+[e_2a_1|l_1d_1]t_m^a), \tag{A16d}$$

where

$$f_{a_1b_2}=h_{a_1b_2}+\sum_{i=i_1,i_2}[ii|a_1b_2]=\sum_{\mu_1\nu_2}\left\{\Psi_{a_1\mu_1}\Psi_{b_2\nu_{21}}t^\perp(\mu_1\nu_2)+\sum_{i=i_1,i_2}\Psi_{i\mu_1}\Psi_{i\mu_1}\Psi_{a_1\mu_1}\Psi_{b_2\nu_2}X^\perp(\mu_1,\nu_2)\right\}. \tag{A17}$$

Then,

$$\sigma_{S/T}^{\mathrm{ET}}=\kappa\left(\frac{C_{1L}+C_{3L}+Z_1}{C'_{1L}-C'_{3L}+Z'_1}\right)\left(\frac{C_{1R}+C_{3R}+Z_2}{C'_{1R}-C'_{3R}+Z'_2}\right), \tag{A18}$$

where S/T denotes singlet/triplet and $\kappa=\langle \mathrm{ex}_S|\mathrm{ex}_S\rangle/\langle \mathrm{ex}_T|\mathrm{ex}_T\rangle$. The C' terms in the denominators are defined in the same way as the C terms in the numerators; the former are evaluated with the triplet exciton wave function $R_\mu(L_\mu)$ and the latter with the singlet.

4. The deductive procedure for $\sigma_{S/T}^{HT}$

The ratio of singlet to triplet cross-section in the large static disorder limit is given for hole transfer (HT) as

$$\sigma_{S/T}^{\mathrm{HT}}=|\langle D_3|H'|D_{1S}\rangle|^2/|\langle D_3|H'|D_{1T}\rangle|^2=\frac{\langle \mathrm{fi}_{1S}|H'|\mathrm{in}_2\rangle\langle \mathrm{in}_2|H'|\mathrm{fi}_{1S}\rangle}{\langle \mathrm{fi}_{1S}|\mathrm{fi}_{1S}\rangle\langle \mathrm{in}_2|\mathrm{in}_2\rangle}\Big/\frac{\langle \mathrm{fi}_{1T}|H'|\mathrm{in}_2\rangle\langle \mathrm{in}_2|H'|\mathrm{fi}_{1T}\rangle}{\langle \mathrm{fi}_{1T}|\mathrm{fi}_{1T}\rangle\langle \mathrm{in}_2|\mathrm{in}_2\rangle}, \tag{A19}$$

where

$$\langle \mathrm{fi}_1|H'|\mathrm{in}_2\rangle = -C_{2L} \pm C_{4L} + Z_3, \tag{A20a}$$

$$\langle \mathrm{in}_2|H'|\mathrm{fi}_1\rangle = -C_{2R} \pm C_{4R} + Z_4. \tag{A20b}$$

The C terms are defined as

$$C_{2L} = \sum_{m_2 e_1 d_1} X_{m_2} U_{d_1 l_1} \{ f_{l_1 m_2} + ([i_1 a_1|l_1 m_2] + [i_2 a_2|l_1 m_2]) t_i^a + [i_1 a_1|b_1 m_2] t_{i_\beta l_\alpha}^{a_\beta b_\alpha} \}, \tag{A21a}$$

$$C_{2R} = \sum_{m_2 e_1 d_1} Y_{m_2} V_{d_1 l_1} \{ f_{l_1 m_2} + ([i_1 a_1|l_1 m_2] + [i_2 a_2|l_1 m_2]) t_i^a + [i_2 a_2|b_2 l_1] t_{i_\beta m_\alpha}^{a_\beta b_\alpha} \}, \tag{A21b}$$

$$C_{4L} = \sum_{m_2 e_1 d_1 l_1} X_{m_2} U_{e_1 l_1} ([d_1 l_1|e_1 m_2] - [i_1 l_1|e_1 m_2] t_i^d + [d_1 a_1|e_1 m_2] t_l^a - [i_1 a_1|e_1 m_2] t_{i_\alpha l_\alpha}^{d_\alpha a_\alpha}), \tag{A21c}$$

$$C_{4R} = \sum_{m_2 e_1 d_1 l_1} Y_{m_2} V_{e_1 l_1} ([l_1 d_1|e_1 m_2] - [m_2 i_1|l_1 d_1] t_i^e + [a_2 e_1|l_1 d_1] t_m^a). \tag{A21d}$$

Then,

$$\sigma_{S/T}^{liT} = \kappa \left(\frac{-C_{2L} + C_{4L} + Z_3}{-C'_{2L} - C'_{4L} + Z'_3} \right) \left(\frac{-C_{2R} + C_{4R} + Z_4}{-C'_{2R} - C'_{4R} + Z'_4} \right). \tag{A22}$$

[1] J. H. Burroughes, D. D. C. Bradley, A. R. Brown, R. N. Marks, K. Mackay, R. H. Friend, P. L. Burn, and A. B. Holmes, Nature (London) **347**, 539 (1990).

[2] G. Gustafsson, Y. Gao, G. M. Treacy, F. Klavetter, N. Colaneri, and A. J. Heeger, Nature (London) **357**, 477 (1992).

[3] R. H. Friend, R. W. Gymer, A. B. Holmes, J. H. Burroughes, R. N. Marks, C. Taliani, D. D. C. Bradley, D. A. Dos Santos, J. L. Brédas, M. Lögdlund, and W. R. Salaneck, Nature (London) **397**, 121 (1999).

[4] N. T. Harrison, G. R. Hayes, R. T. Phillips, and R. H. Friend, Phys. Rev. Lett. **77**, 1881 (1996).

[5] H. Becker, S. E. Burns, and R. H. Friend, Phys. Rev. B **56**, 1893 (1997).

[6] F. Garten, A. Hilberer, F. Cacialli, F. Esselink, Y. Van-Dam, B. Schlatmann, R. H. Friend, T. Klapwijk, and G. Hadziioannou, Adv. Mater. **9**, 127 (1997).

[7] A. R. Brown, D. D. C. Bradley, J. H. Burroughes, R. H. Friend, N. C. Greenham, P. L. Burn, A. B. Holmes, and A. Kraft, Appl. Phys. Lett. **61**, 2793 (1992).

[8] Y. Cao, I. Parker, G. Yu, C. Zhang, and A. J. Heeger, Nature (London) **397**, 414 (1999).

[9] P. K. H. Ho, J. S. Kim, J. H. Burroughes, H. Becker, S. F. Y. Li, T. M. Brown, F. Cacialli, and R. H. Friend, Nature (London) **404**, 481 (2000).

[10] M. Wohlgenannt, K. Tandon, S. Mazumdar, S. Ramasesha, and Z. V. Vardeny, Nature (London) **409**, 494 (2001).

[11] Z. Shuai, D. Beljonne, R. Silbey, and J. L. Brédas, Phys. Rev. Lett. **84**, 131 (2000).

[12] M. Kobrak and E. Bittner, J. Chem. Phys. **112**, 5399 (2000).

[13] M. Kobrak and E. Bittner, J. Chem. Phys. **112**, 5410 (2000).

[14] M. Kobrak and E. Bittner, Phys. Rev. B **62**, 11 473 (2000).

[15] D. Beljonne, Z. Shuai, R. H. Friend, and J. L. Brédas, J. Chem. Phys. **102**, 2042 (1995).

[16] A. L. Bunn and M. A. Ratner, J. Chem. Phys. **109**, 6092 (1998).

[17] L. Hulthen and M. Sugawara, *Handbuch der Physik* (Springer-Verlag, Berlin, 1957), Bd. **39**, p. 1.

[18] J. Cizek and J. Paldus, Phys. Scr. **21**, 251 (1980).

[19] R. J. Bartlett, Annu. Rev. Phys. Chem. **32**, 359 (1981).

[20] G. D. Purvis III and R. J. Bartlett, J. Chem. Phys. **76**, 1910 (1982).

[21] R. J. Bartlett, J. Phys. Chem. **93**, 169 (1989).

[22] Z. Zhuai and J. L. Brédas, Phys. Rev. B **62**, 15 452 (2000).

[23] A. C. Scheiner, Q. E. Scuseria, J. E. Rice, T. J. Lee, and H. F. Schaeffer, J. Chem. Phys. **87**, 5361 (1987).

[24] K. Ohno, Theor. Chim. Acta **2**, 219 (1964).

[25] G. Klopman, J. Am. Chem. Soc. **86**, 4550 (1964).

[26] S. Kivelson, W. P. Su, J. R. Schrieffer, and A. J. Heeger, Phys. Rev. Lett. **58**, 1899 (1987).

[27] D. K. Campbell, J. T. Gammel, and E. Y. Loh, Jr., Phys. Rev. B **42**, 475 (1990).

[28] A. Painelli and A. Girlando, Solid State Commun. **66**, 274 (1988).

[29] M. J. Rice and Yu. N. Gartstein, Phys. Rev. B **53**, 10 764 (1996).

[30] P. W. M. Blom, M. J. M. de Jong, and J. J. M. Vleggaar, Appl. Phys. Lett. **68**, 3308 (1996).

[31] H. Antoniades, M. A. Abkowitz, and B. R. Hsieh, Appl. Phys. Lett. **65**, 2030 (1994).

[32] Z. G. Soos and S. Ramasesha, Phys. Rev. B **29**, 5410 (1984).